Journal of Ovonic Research Vol. 16, No. 6, November - December 2020, p. 345 - 353

PREPARATION AND INVESTIGATIONS OF STRUCTURAL, OPTICAL AND CONDUCTIVITY PROPERTIES OF POLYANILINE/TITANIUM DIOXIDE NANOCOMPOSITES

S. C. VELLA DURAI[a,*], E. KUMAR[b], R. INDIRA[c], D. MUTHURAJ[d]
[a*]*Department of Physics, JP College of Arts and Science, Agarakattu, Tenkasi, Tamilnadu, India*
[b]*School of Science, Department of Physics, Tamil Nadu Open University, Chennai. Tamilnadu, India*
[c]*Department of Chemistry, SDNB Vaishnav College for Women, Chromepet, Chennai. Tamilnadu, India*
[d]*PG and Research Department of Physics, The M.D.T Hindu College, Tirunelveli. Tamilnadu, India*

Nanocomposites of polyaniline (PANI) encapsulating titanium dioxide (TiO_2) nanoparticles (NPs) were prepared by in-situ polymerization method in the presence of TiO_2 NPs. The prepared nanocomposites were analyzed by powder X-ray diffraction (P-XRD), uv-visible absorption spectroscopy (UV), Fourier-transform infrared spectra (FTIR) and high resolution transmission electron microscope (HRTEM). An AC conductivity study of PANI/TiO_2 nanocomposites was analyzing in between 1 Hz to 8 MHz and a particular temperature 50^0C. The P-XRD was explaining amorphous nature in PANI/TiO_2 nanocomposites respectively. The particle size was observed and confirmed using HRTEM, which shows the formation of nanocomposites at around near in spherical shape in the nanoscale range. An FTIR study confirms the bonding and formation of the prepared samples. FTIR spectral obtained shows that TiO_2 and PANI NPs are not simply encapsulated and a strong interaction obtain at the interface of PANI and TiO_2 NPs. A UV- vis spectra was used to analysis the confined polymerization process of PANI doped TiO_2. The UV absorption spectrum showed a blue shift as compared to the pure TiO_2 NPs. AC conductivity measured indicates that the conductivity of PANI/TiO_2 nanocomposites is decreased with TiO_2 NPs. The AC conductivity of PANI/TiO_2 nanocomposites has measured at a 146 S cm^{-1}. The AC conductivity property is obtained to be changed due to the combine of TiO_2 NPs, which induced the formation of a coherent for charging transport in the base PANI chain.

(Received August 3, 2020; Accepted November 2, 2020)

Keywords: Absorbance, Band gap, Conductivity, Crystalline, Nanocomposites

1. Introduction

A nanocomposite is a notable type of new materials having individual properties of physical, chemical concepts and many high potential applications in new devices. Good applications of nanocomposites materials can be change by the mixed the properties of bulk parent materials into nano size material [1]. Doping of semiconducting NPs inside to the high conducting PANI chain, have a very interesting concept of nanocomposites preparation [2]. When different metal oxide NPs has been doped to the chain of good conducting polymers, it's converted to nanocomposite materials [3]. This nanocomposites material is different from the pure semiconductor and polymer in chemical and physical properties [4, 5]. The polymer is insoluble in common solvents, and in fusible. Therefore, preparation method has to be searched and analyzed, and confirms to combine with the semiconductor NPs and polymers [6].

Semiconducting nano materials can be combining with polymers by some special chemical technique incorporation method. Entire conducting polymers, PANI have individual properties due to the presence of –NH– groups in a polymer chain edge, on both sides by

* Corresponding author: duraipree@gmail.com

phenylene rings. PANI has chemical flexibility and increase itself due to the process, ability to a large area [7]. PANI is good conducting polymers; due to it have good electrical conductivity, high environmental stability and high potential application in nano devices. Optical behaviour of PANI can be changed by mixed of semiconducting nanomaterials [8]. Nanoscale materials have important behaviour, due to mysterious nature arising from the large surface area. The encapsulation of nano size materials may be improved the structural, optical (band gap) and electrical properties of PANI materials [9]. Some research articles reported that the AC conductivity property of PANI/TiO_2 nanocomposites with a low TiO_2 is higher than of pure PANI [10-12]. Other some research article also noticed that the PANI/TiO_2 nanocomposites have good structural, optical, conductivity, and dielectric properties [13-15]. The reason for the good structural, optical, and electrical studies of nanocomposites is not constant and clear.

In this paper, we explain the characteristics of PANI/TiO_2 nanocomposites. PANI/TiO_2 nanocomposite combines the pure PANI and TiO_2 NPs and has high potential application in a like charge storage, photovoltaic properties, conductive coating, electro catalytic applications and absorptions material of solar cell. In these article results indicate that pure PANI and TiO_2 NPs are not simply added, TiO_2 NPs act as the reaction core, and a strong interaction exists at the interface of pure PANI and TiO_2 NPs. The structural, optical, and electrical property of PANI/TiO_2 nanocomposite was characterized. Enhanced, but not constant, amorphous structure was observed.

2. Materials and methods

2.1. Materials

Chemicals are used in this preparation, are titanium tetra isopropoxide (TTIP), acetic acid, aniline, Ammonium per sulphate (APS), HCl, TiO_2 NPs and deionized water.

2.2. TiO_2 NPs preparation

TiO_2 NPs preparation by microwave assisted solution method as below: The first solution is prepared by 25 ml deionize water mixed with 2.5 ml of acetic acid. The second solution is prepared by 5.8 ml of titanium tetra isopropoxide (TTIP) was mixed with 20ml deionized water. The first prepared solution is mixed with the in drop wise second prepared solution during stirring, stirred in continuously for 4 hours, and got a clear white colour solution. After 1 hour, the solution was kept in a micro oven at 40 °C for 15 min. Then solution was filtered, and dried at 60 °C, and get a white colour TiO_2 NPs. Prepared NPs were crushed into fine powder with mortar.

2.3. PANI NPs preparation

4.5ml aniline was mixed with 70ml of hydrochloric solution. After 6 hours, 4.5 grams of APS were dissolved in 20 ml deionized water, and its added drop wise in a controlled solution with the constant stirring. The polymerization was developed at 60^0C. The reaction solution was filtered, washed with 2M HCl and de-ionized water. Afterwards, it is dried at 100^0 C in the vacuum for two days, and to get a green fine powder.

2.4. PANI / TiO_2 nanocomposites (5wt %) preparation

Five weight percentages of PANI/TiO_2 nanocomposites were synthesized by in situ polymerization methods as follows: 4.5ml aniline was injected into 70ml of HCl (2M) which contains TiO_2 NPs of 0.09g (5 weight percentages). After two hours, 4.5 g of APS was taken and dissolved in 20 ml deionized water. Here, the both prepared solution is mixed to drop wisely and stirred at 40^oC for 60 min. The reaction solution was filtered, washed with two moralities HCl and deionized water. Afterwards, it is dried at room temperature in the vacuum for one day to obtain a green powder.

2.5. Experimental

The Powder XRD was characterized using powder X-ray diffractometer (XPERT-PRO uses CuKα1, λ=0.1540 nm radiation). The formation of nanocomposite was carried out the High Resolution Transmission Electron Microscope using JOEL JEM 2000. The powder sample was

recorded by FT-IR spectrum using FTIR (JASCO FTIR-4100) in range of wavelengths as 400 to 4000 cm^{-1}. The sample was recorded the optical spectrum using UV Visible spectroscopy (UV-2600) in range of wave number as 200-1200 cm^{-1}. The AC conductivity was recorded in the frequency range of 1 Hz to 8 MHz by impedance spectroscopy (Zahnner zennium IM6 meter).

3. Results and discussion

3.1. Powder X-Ray Diffraction analysis

Fig. 1 shows that, powder X-ray diffraction images for pure PANI, TiO_2 and PANI/TiO_2 nanocomposites material. The TiO_2 NPs peaks (Fig. 1 (b)) appeared 2θ value at 25.2854°, 37.8654°, 47.8217°, 53.3905°, 62.4606°, and 68.8698° correlates the millar indices of (101), (004), (200), (105), (213), and (116). The high intense peaks are 25.2854°, 37.8654°, 47.8217° with d spacing 3.5181 Å, 2.3732 Å, and 1.8998 Å. This peak indicates the TiO_2 confirms the degree of crystalline, which is confirmed with JCPDS card number 21-1272 [16]. The P-XRD patterns correlates with the same articles explain and confirm the preparation of TiO_2 NPs. The peak value of 25.3075°, which is the more peak for TiO_2 NPs and correlated crystalline plane, was (101). The prepared TiO_2 nanoparticle was crystalline, and the crystalline size was observed from scherrer equation [17],

$$D = 0.9\lambda / \beta Cos\theta$$

where λ is the wavelength and D is the crystallite, β-is the full FWHM (width at half maximum height) of the XRD peak. The average crystalline size calculated for the prepared TiO_2 nanoparticle was around 12 nm. The pure PANI peaks show that a small peak is around 2θ = 15.0244, 20.4200 and 25.2451, with a d spacing 5. 8897 Å, 4.3440 Å and 3.5236 Å indicating the conducting PANI also confirm the low crystalline structure [18]. The crystalline size of the PANI is around 11 nm which was calculated from scherrer equation.

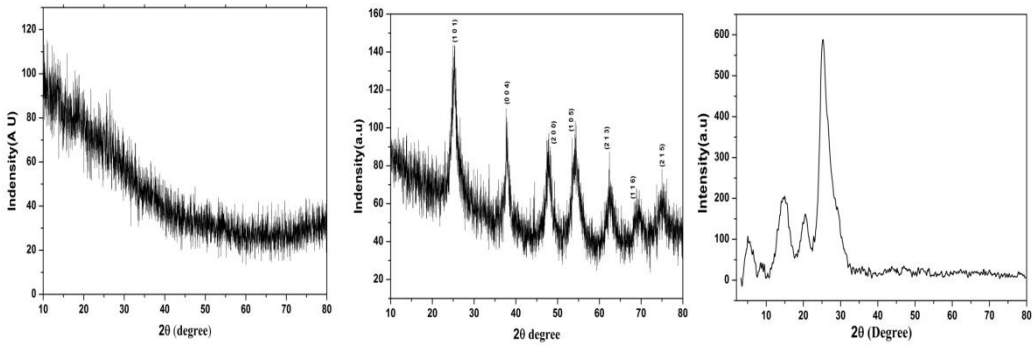

(a) *(b)* *(c)*

Fig. 1. Powder XRD pattern of a) PANI/TiO_2 Nanocomposites, b) Pure TiO_2, and c) Pure PANI NPs.

For PANI/TiO_2 nanocomposite, the peak of the pure TiO_2 NPs phase is not clear but could not be observed peaks as shown (Fig. 1 (a)) and it indicates the amorphous nature of nanocomposites. PANI is crystalline in structure (Fig. 1 (c)) which may be allocated the scattering of PANI chain at d spacing. When ammonium per sulfate is mixed to the preparation technique, it is obtained that polymerization taking initially on the surface of TiO_2 NPs due to the restrictive effect of the surface. Thereafter, crystalline PANI combines the crystalline behaviors of TiO_2 NPs thus obtain its amorphous structure. Therefore, the degree of crystalline of PANI decreases, and the x-ray diffraction peaks revealed, combine and decreased with TiO_2 NPs peaks, and hence, cannot be distinguished [19]. Comparing pure TiO_2, pure PANI with nanocomposites, it is clear that XRD of the PANI/TiO_2 nanocomposites are not identical of crystalline structure to those of TiO_2 NPs. These explain that PANI polymerization of TiO_2 NPs has effect on the crystallization

performance of nanocomposites materials. However, nanocomposite was explained, which explain the amorphous nature of nanocomposites.

3.2. High Resolution Transmission Electron Microscope Analysis

Fig. 2 shows the HRTEM images of PANI/TiO_2 nanocomposite with 5 wt% of TiO_2 nanocomposite with different magnification. The white area and black core of Fig. 2 (a) explain the PANI chain and TiO_2 NPs respectively. It is shown from the Fig. 2 (a & b) and it has TiO_2 NPs are well-encapsulated into the PANI chain. The PANI chain clearly revealed that the have TiO_2 NPs (black core), due to encapsulation in TiO_2 NPs with the PANI chain. For Fig. 2 (c) shows HRTEM image higher magnification, and it also shows that the irregular arranged NPs within the PANI matrix. Fig. 2 (d). Shows that the selected area electron diffraction pattern (SAED) of PANI/TiO_2 nanocomposites. The amorphous structures of the nanocomposites leads to it have a corresponding less pronounced diffuse rings in the SAED pattern [20]. However, when the 5 wt % TiO_2 NPs concentration, there is not regular arrangement of NPs can be observed. The PANI/TiO_2 nanocomposite morphology could be change, is due to the formation of clusters in the morphology or some kind of pressure have developed during the polymerization. The particle size was observed and confirmed using HRTEM, which shows the formation of nanocomposites at around spherical shape in the nanoscale range. The result of HRTEM image is reported that the nanocomposite is combined of TiO_2 NPs and PANI, which is in compatibility with the results measured by XRD analysis [21].

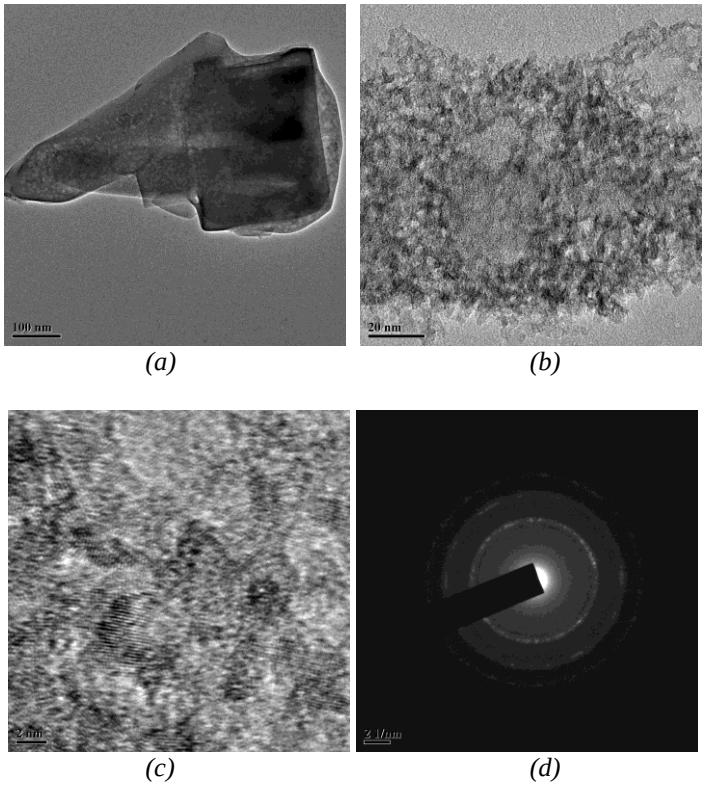

(a) *(b)*

(c) *(d)*

Fig. 2. HRTEM images of PANI/TiO_2 Nanocomposites

3.3. Fourier Transform Infra-Red spectroscopy (FTIR) Analysis

In Fig. 3 (a, b, and c) FTIR analyses of the PANI/ TiO_2 nanocomposites, TiO_2 and PANI NPs showed the formation of phase purity materials. The main characteristic peak of pure TiO_2 is assigned as followed: the peak at 581 cm^{-1} is attributable to Ti-O-O vibration bond, and it is indicates the formation of a titanium dioxide [22]. A broad peak at 3207 cm^{-1}, peak is associated with hydroxyl groups. The peak at 1616 cm^{-1} is due to the bending vibrations of the -OH groups, and peak at 1490 cm^{-1} is a stretching vibration of Ti-O-Ti [23]. It observed of various well-defined

peaks are 3882, 3828, 1299, 1143, and 737 cm^{-1}. The characteristic peak of PANI is assigned as followed: the broad peak 3486 cm^{-1} is assigned to N-H stretching vibrations of secondary amine, and sharp peaks at 1540 cm^{-1} is also assigned to C=C stretching of quinoid ring (N=Q=N). The peak 1465 cm^{-1} is attributable to C=C stretching vibration of benzenoid ring (N-B-N), and 1300 cm^{-1} is attributable to C - N stretching of the secondary aromatic ring. The peak 1121 cm^{-1} is corresponding to aromatic C–H in-plane bending vibrations, 812 cm^{-1} and 508 cm^{-1} are attributed to aromatic C–H out-of-plane bending vibrations. These all peaks positions match well with those results in the same research articles [24-26].

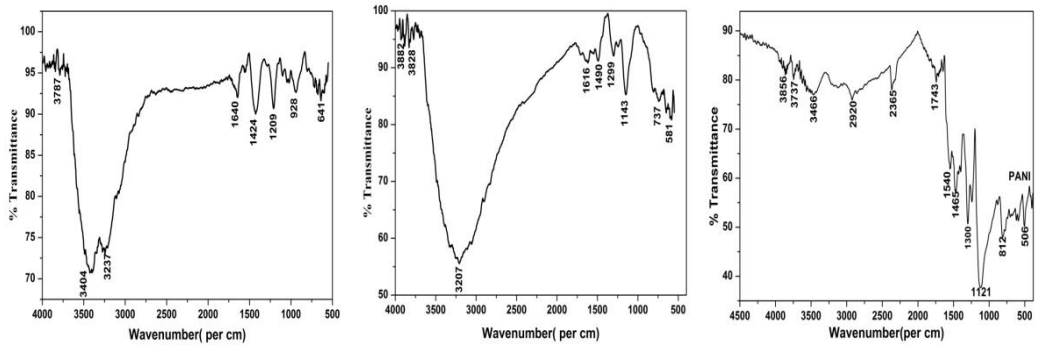

(a) *(b)* *(c)*

Fig. 3. FTIR pattern of a) PANI/TiO_2 Nanocomposites, b) Pure TiO_2, and c) Pure PANI NPs

The characteristics peak of PANI/TiO_2 is assigned as followed: the peak at 928 cm^{-1} is assigned to plane bending vibrations of C-H which are found during protonation [27]. The vibration bond is 3237 cm^{-1} due to the NH stretching of aromatic amines, is 641 cm^{-1} due to CH out of the plane bending vibrations. The CH out of the plane bending has been used to indicate the substituted benzene. A broad peak at 3404 cm^{-1}, is associated with hydroxyl groups. The peak at 1424 cm^{-1} is assigned to C=C stretching mode of vibrations for benzenoid units of PANI. The peak at 1209 cm^{-1} is obtained to the C-N stretching modes of the benzenoid ring. The peak at 1209 cm^{-1} is the analysis of the conducting protonated form of PANI [28]. The peaks at 641 cm^{-1} develops from the out of plane C-H bending vibrations. The less wavenumber regions explain vibrations 641 cm^{-1} which corresponds to the anti-symmetric Ti-O-Ti mode of the titanium dioxide. It observed of various well-defined peaks are 3787, 1640, and 928 cm^{-1}.This peak when compared to that of PANI [29] is found to be shift due to strong attraction of pure TiO_2 nanoparticle with PANI. Similar observations have been reported by some article [30]. This result shows that. It was confirmed the organic and inorganic compounds present in the prepared samples.

3.4. UV Visible spectroscopy Analysis

UV-Visible absorption spectrum of PANI/TiO_2 nanocomposites pure TiO_2 and pure PANI are shown in Fig. 4. Pure TiO_2 and PANI NPs show an absorbance peak at 325 and 253 nm, it means that they explain good absorbance at UV region. The UV-Vis absorption spectra of TiO_2 doped PANI show a peak at 235 nm. Some change was obtained in the shape of the UV-vis spectrum in the spectrum regions, the change in the peak with encapsulation of TiO_2 NPs in PANI chain which is due to nice absorption studies of TiO_2 NPs [31, 32].

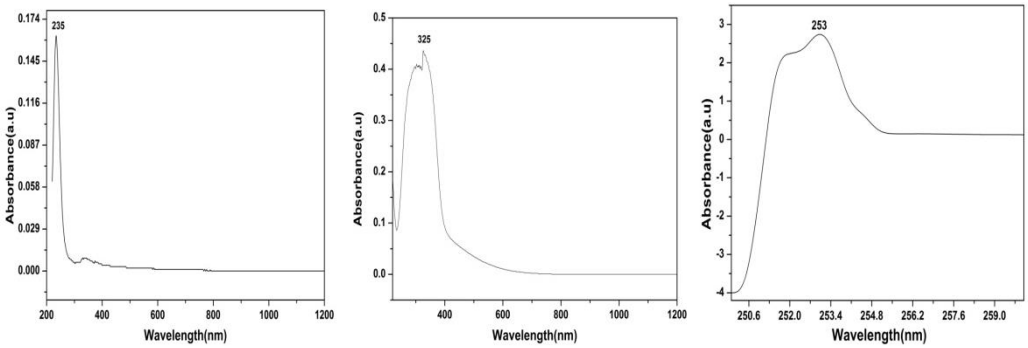

(a) *(b)* *(c)*

Fig. 4. UV pattern of a) PANI/TiO_2 Nanocomposites, b) Pure TiO_2, and c) Pure PANI NPs

This peak at 235 nm corresponds to the π-π* electronic transition which represents the presence of TiO_2 NPs. Moreover, The absorption peak of TiO_2 NPs at 375 nm shifted to a lower wavelength (blue shift) after encapsulation with PANI (5wt%) showing the absorption peak at 235 nm. After encapsulation with PANI the response of TiO_2 to visible area was decreased and showed the blue shift (towards the decreased wavelength) [33]. It confirms that encapsulations of TiO_2 NPs have the effects on the doping of pure PANI chain, while this effect should be to an interaction at the interface of PANI and TiO_2 NPs [34, 35].

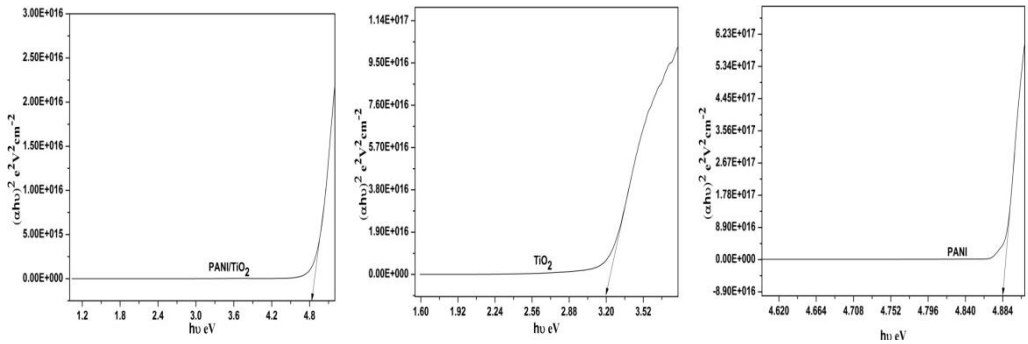

(a) *(b)* *(c)*

Fig. 5. Band gap plot of a) PANI/TiO_2 Nanocomposites, b) Pure TiO_2, and c) Pure PANI NPs

The optical band gap is observed to Tauc's plot from UV-Vis absorption spectrum using the following equation. [36]

$$\alpha h\gamma = A\,(h\gamma - E_g)^n$$

where E_g is the band gap, γ is the frequency of light, h is Planck's constant, α is the absorption coefficient, 'n' is 1/2 for a direct transition, and 2 for an indirect transition and A is a constant. Fig. 5 shows a Tauc's plot and band gap for pure TiO_2, PANI and PANI/TiO_2 nanocomposites. Tauc plots is plotted in between hν and $(\alpha h\nu)^2$. The straight line of the plot (hν vs $(\alpha h\nu)^2$ to $\alpha = 0$) may be obtained by band gap energy. The band gap of pure PANI is measured at 4.88 eV, and a decrease in the band gap energy with the encapsulation of TiO_2 is also observed from 4.83 eV with 5 % TiO_2 which are obtained the higher band gap of TiO_2. The band gap of pure TiO_2 is measured at 4.88 eV, which is similar to some research article reports [37]. The changes in the band gap energy is a marking of changed absorbance of coordinate complex formed between TiO_2 and PANI chain, which is explaining a decreasing due to high concentration of TiO_2 NPs in nanocomposites [38, 39].

3.5. AC Conductivity Analysis

Fig. 6 (a, b, and c) shows that AC conductivity (σ_{ac}) as a function of angular frequency at a particular temperature (50^{o}C) for PANI/TiO_2 nanocomposites (5 wt %), pure PANI and TiO_2 NPs. The pure TiO_2 and PANI NPs σ_{ac} are 822 and 3126 (S per cm) at higher angular frequency regions respectively in a particular temperature. Prepared NPs are obtained that, NPs σ_{ac} are remains constant up to frequency 3 (radian per second) and thereafter increases slowly, which properties nature of ordered materials are. At high angular frequency regions, σ_{ac} is increases because of distribution of regularly arranged charge particles.

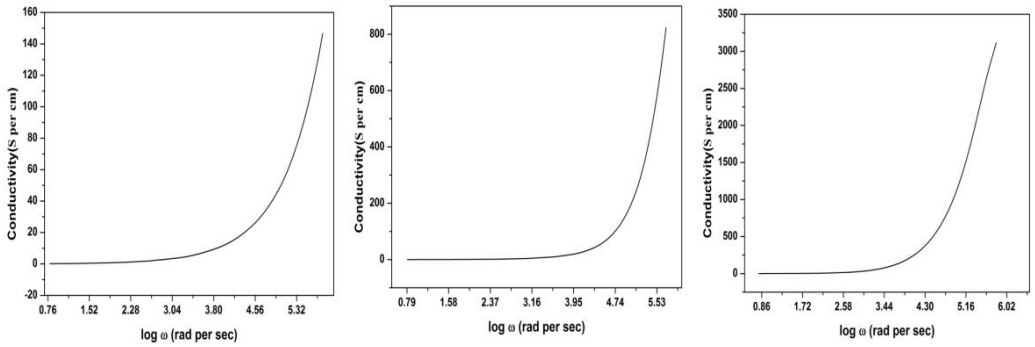

Fig. 6. Conductivity image of a) PANI/TiO_2 Nanocomposites, b) Pure TiO_2, and c) Pure PANI NPs

Prepared nanocomposites is measured that in the nanocomposites σ_{ac} remains unchanged frequency up to 3.12 (radian per second) and thereafter increases slowly, which properties nature of disordered materials are. At high angular frequency regions, σ_{ac} increase because of distribution of polaron, which is moving with smaller distance in a polymer chain. [40]. The σ_{ac} is increases at high-frequency regions, is due to the motion of charge in the amorphous region, and it confirms the presence of isolated polaron in these regions. The conductivity of the nanocomposites is 147 (S per cm), it is very lowing conductivity compared to pure PANI and TiO_2 NPs. Which is the reason for low conductivity in high weight percentage of TiO_2 NPs in PANI may be due to TiO_2 NPs, blocking the conduction way in PANI chain. These nanocomposites explain and confirm to a maximum number of polarons where polaron coupling getting gradually stronger even though irregular arrangement, explaining to severe pinning of polaron, thus restricting their distribution at higher angular frequency, hence confirmed in decreasing of conductivity [41].

4. Conclusion

In conclusion, PANI/TiO_2 nanocomposites with five weights percentages of TiO2 NPs were successfully prepared by in-situ polymerization method. The characteristics of PANI/TiO_2 by powder XRD, FTIR, UV-vis, and electrical conductivity confirm the presence of PANI and TiO_2 NPs in the nanocomposite materials. From the HRTEM images and powder X-ray diffraction, it was identified that the TiO_2 NPs form a relatively irregular distribution in the PANI chain. The nanocomposite results were obtained with FTIR studies which confirmed the formation of PANI/TiO_2 nanocomposites. The absorption peaks in UV-vis spectrum of PANi/TiO_2 nanocomposites were found to blue shift to a lower wavelength as compared to those measured in pure PANI. The observed blue shift was attributed to the interaction between the TiO_2 NPs and PANI chains. The band gap nanocomposites is also observed from 4.83 eV with 5 % TiO_2 which is obtained the higher band gap of TiO_2. The AC conductivity nanocomposites were decreased which confirms the formation of a lesser charge distribution in the conducting PANI chain.

Acknowledgements

The author are thankful to high authorities of JP College of Arts and Science, Agarakattu, Tenkasi for providing necessary research facilities.

References

[1] P. H. C. Camargo, K. G. Satyanarayana, F. Wypych, Mat. Res. **12**(1), 1 (2009).
[2] S. Li, M. M. Lin, M. S. Toprak, D. K. Kim, M. Muhammed, Nano Rev. **1**(1), 5214 (2010).
[3] S. Vyas, S. Shivhare, A. Shukla, International Journal of Research and Scientific Innovation **4**(7), 86 (2017).
[4] R. Gangopadhyay, A. De, Chem. Mater. **12**, 608 (2000).
[5] T. H. Le, Y. Kim, H. Yoon, Polymers **9**(150), 1 (2017).
[6] M. Tomczykowa, M. E. P. Brzezinska, Polymers **11**(2), 350 (2019).
[7] T. Yonehara, K. Komaba, H. Goto, Polymers **12**(2), 375 **(***2020*).
[8] M. Khairy, M. E. Gouda, J. Adv. Res. **6**(4), 555 (2015).
[9] S. M. Reda, S. M. Al-Ghannam, Advances in Materials Physics and Chemistry **2**, 75 (2012).
[10] T. C. Mo, H. W. Wang, S. Y. Chen, Y. C. Yeh, Ceram. Int. **34**, 1767 (2008).
[11] I. B. Abbes, E. Srasra, J. Nanomater. **516902**, 1 (2015).
[12] M. Irfan, A. Shakoor, B. Ali, A. Elahi, Tahira, M. I. Ghouri, A. Ali, European Academic Research **2**(8), 10602 (2014).
[13] A. M. Al Baradi, S. F. Al Shehri, A. Badawi, A. Merazga, A. A. Atta, Results Phys. **9**, 879 (2018).
[14] N. S. Kumar, S. K. N. Kumar, L. Yesappa, Mater. Res. Express **7**(1), 015071 (2020).
[15] A. M. Meftah, E. Gharibshahi, N. Soltani, W. M. M. Yunus, E. Saion, Polymers **6**(9), 2435(2014).
[16] S. Ramalingam, International Journal of Innovative Technology and Exploring Engineering **9**(2S2), 732 (2019).
[17] S. C. Vella Durai, E. Kumar, D. Muthuraj, V. Bena Jothy, Int. J. Nano Dimens. **10**(4), 454 (2019).
[18] A. Mostafaei, A. Zolriasatein, Progress in Natural Science: Materials International **22**(4), 273 (2012).
[20] P. Rajakani, C. Vedhi, Int. J. Ind. Chem. **6,** 247 (2015).
[21] D. C. Manatunga, R. M. De Silva, K. M. N. De Silva, N. De Silva, E. V. A. Premalal, R. Soc. open sci. **5**, 171557 (2018).
[22] M. T. Ramesan, V. Nidhisha, P. Jayakrishnan, Materials Science in Semiconductor Processing **63,** 253 (2017).
[23] G. Rajakumar, A. A. Rahumana, S. M. Roopan, V. G. Khanna, G. Elango, C. Kamaraj, A. A. Zahir, K. Velayutham, Spectrochim. Acta Part A **91**, 23 (2012).
[24] T. Kavitha. A. Rajendran, A. Durairajan. International Journal of Emerging Technology and Advanced Engineering **3**(1), 636 (2013).
[25] Ebogodi, K. Otlhao, Klink. Asian J. Chem. **29**(6), 1206 (2017).
[26] K. Zhang, L. L. Zhang, X. S. Zhao, J. Wu, Chem. Mater. **22**(4), 1392 (2010).
[27] S. Goswami, U. N. Maiti, S. Maiti, S. Nandy, M. K. Mitra, K. K. Chattopadhyay, Carbon **49**(7), 2245 (2011).
[28] E. T. Kang, K. G. Neho, K. L. Tan, Prog. Polym. Sci. **23**, 277 (1998).
[29] S. G. Pawar, S. L. Patil, M. A. Chougule, S .N. Achary, V. B. Patil, Int J. Polym. Mater. **60,** 244 (2011).
[30] T. Ozawa, Thermochim. Acta. **203,** 159 (1992).
[31] I. S. Lee, J. Y. Lee, J. H. Sung, H. J. Choi, Synth. Met. **152**(1-3), 173 (2005).
[32] X. Ma, M. Wang, G. Li, H. Chen, R. Bai, Mater. Chem. Phys, **98**(2-3), 241 (2006).
[33] R. Sainz, W. R. Small, N. A. Young, C. Valles, A. M. Benito, W. K. Maser, M. H. Panhuis, Macromolecules **39**(21), 7324 (2006).
[34] S. Kumar, N. K. Vermaa, M. L. Singlab, Digest Journal of Nanomaterials and Biostructures

7(2), 607 (2012).
[35] X. Li, G. Wang, X. Li, D. Lu, Appl. Surf. Sci. **229**(1-4), 395 (2004).
[36] S. Srivastava, S. Kumar, V. N. Singh, M. Singh, Y. K. Vijay, Int. J. Hydrogen Energy **36**(10), 6343(2011).
[37] A. K. Sharma, R. Vyas, P. K. Jain, U. Chand, V. K. Jain, J. Nano-Electron. Phys. **11**(2), 2012 (2019).
[38] C. Dette, M. A. P. Osorio, C. S. Kley, P. Punke, C. E. Patrick, P. Jacobson, K. Kern, Nano Lett. **14**(11), 6533 (2014).
[39] R. Cruz-Silva, J. Romero-Garcia, J. L. Angulo-Sanchez, E. Flores-Loyola E, M. H. Farias, F. F. Castillon, Polymer. **45**(14), 4711 (2004).
[40] X. Li, G. Wang, D. Lu, Appl. Surf. Sci. **229**(1-4), 395 (2004).
[41] V. S. Chaturmukha, C. S. Naveen, M. P. Rajeeva, B. S. Avinash, H. S. Jayanna, A. R. Lamani, American Institute of Physics **1731**, 050066 (2016).
[42] S. J. Su, Kuramoto, Synth. Met. **114**(2), 147 (2000).